HHS Public Access

Author manuscript

Inorg Chem. Author manuscript; available in PMC 2017 March 07.

Published in final edited form as:

Inorg Chem. 2016 March 07; 55(5): 1962–1969. doi:10.1021/acs.inorgchem.5b02036.

Fluorophore Assisted Photolysis of Thiolato-Cob(III)alamins

Zachary L. Rodgers[†], **Thomas A. Shell**[‡,‖], **Alexander M. Brugh**[†], **Hannah L. Nowotarski**[†], **Malcolm D. E. Forbes**[†,⊥], and **David S. Lawrence**[†,‡,§,*]

[†]Department of Chemistry, University of North Carolina, Chapel Hill, North Carolina 27599, United States

[‡]Division of Chemical Biology and Medicinal Chemistry, University of North Carolina, Chapel Hill, North Carolina 27599, United States

[§]Department of Pharmacology, University of North Carolina, Chapel Hill, North Carolina 27599, United States

Abstract

Cobalamins are known to react with thiols to yield stable β-axial Co^{III}–S bonded thiolato-cobalamin complexes. However, in stark contrast to the Co–C bond in alkylcobalamins, the photolability of the Co–S bond in thiolato-cobalamins remains undetermined. We have investigated the photolysis of *N*-acetylcysteinyl cob(III)alamin at several wavelengths within the ultraviolet and visible spectrum. To aid in photolysis, we show that attaching fluorophore "antennae" to the cobalamin scaffold can improve photolytic efficiency by up to an order of magnitude. Additionally, electron paramagnetic resonance confirms previous conjectures that the photolysis of thiolato-cobalamins at wavelengths as long as 546 nm produces thiyl radicals.

Graphical Abstract

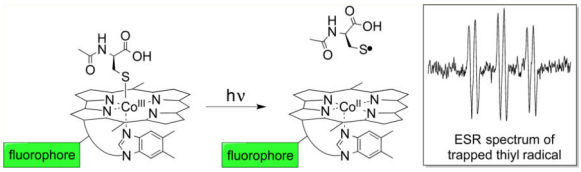

[*]**Corresponding Author**. lawrencd@email.unc.edu.

[‖]**Present Addresses**

Department of Chemistry, Saint Anselm College, Manchester, New Hampshire 03102, United States.

[⊥]Department of Chemistry, Bowling Green State University, Bowling Green, Ohio 43403, United States.

ASSOCIATED CONTENT

Supporting Information

The Supporting Information is available free of charge on the ACS Publications website at DOI: 10.1021/acs.inorgchem.5b02036.

Scheme; figures of LC-MS chromatograms, photoinduced conversion of **NAcSCbl, NAcSCbl-1–4, MeCbl**, and absorption spectra; and table of quantum yield, extinction coefficients, efficiency, and reaction rate constants (PDF)

The authors declare no competing financial interest.

INTRODUCTION

The cobalamins (Cbls), which comprise the various forms of vitamin B_{12}, are cobalt corrinoids necessary for sustaining life.[1,2] These structurally complex entities contain a low spin (d^6) Co^{III} ion equatorially coordinated by a macrocyclic corrin ring system and axially bound by a dimethylbenzimidazole nucleotide. The β-axial site can accommodate a variety of ligands, but in the cell, alkylCbls with methyl (**MeCbl**) and adenosyl ligands provide the bioactive forms. In addition to their biological importance, alkylCbls display intriguing photochemistry that has been the subject of extensive studies since the 1960s.[3,4] These complexes contain a weak Co–C bond with a ground state, homolytic bond dissociation energy estimated by various methods to be between 30 and 44 kcal/mol.[1,5–9] Upon absorption of visible light (<600 nm), these complexes undergo homolytic scission to yield a Co^{II} and alkyl radical pair. The absorptive transition occurring within these complexes is thought to arise from an initial metal-to-ligand and σ-bond-to-ligand charge transfer between the axial ligands ($N_{imidazole}$-Co-C) and the corrin ring.[10–14] However, new theoretical studies have implicated ligand field transitions on the path to homolytic scission in **MeCbl** as well.[15,16] AlkylCbls display remarkable photolability with observed, aerobic quantum yields (Φ, reactions per photon absorbed) of photolysis (ligand release) as high as 30%.[3]

Cbls react with a wide array of mercaptans to provide stable, β-axial Co–S bonded complexes known as thiolato-Cbls.[17–19] However, in contrast to the extensive photolytic studies on alkylCbls, investigations of thiolato-Cbl photolability are quite limited. Indeed, although several studies reference a general sensitivity of thiolato-Cbls toward light, they typically expound no further on the issue.[1,19–21] Furthermore, although there is a general sense that thiolato-Cbls are more resistant to photolysis than alkylCbls, the similar spectra produced by both thiolato-Cbl and alkylCbls, especially in the γ absorption band (300–400 nm), indicate possible commonalities in bonding and electronic transitions (Figure 1). For example, both the Co–C and the Co–S bonds in alkylCbls and thiolato-Cbls, respectively, display similar charge transfer and bonding interactions.[22,23] In short, the information available to date supports the notion that thiolato-Cbls should suffer photolysis in a fashion not unlike their alkylCbl counterparts (however, *vide infra*).[22]

Our interest in the photosusceptibility of thiolato-Cbls derives from the utility of alkylCbls as light-responsive agents for drug delivery and in the preparation of polymeric materials.[24–29] Furthermore, we have demonstrated that long wavelength “antennas”, appended to the Cbl, can be used to capture light in the red, far red, and near-IR, resulting in photolytic release of biologically active agents.[30] However, although the remarkably high Φ associated with alkylCbls allows for facile photocleavage, their extreme light sensitivity can complicate the handling and fluorescent imaging of these derivatives.[29,30] Consequently, we decided to explore the photolability of thiolato-Cbls, as well as the modulation of thiolato-Cbl photosensitivity, with the expectation that constructs less photosensitive than alkylCbls may be useful in the photodelivery of therapeutic agents.

EXPERIMENTAL SECTION

Potential Hazards

Hg arc lamps emit high intensity ultraviolet light, and therefore, shaded ultraviolet eye protection is required.

Materials and Methods

Alexa Fluor 350 (Alexa350) was purchased from Life Technologies, 7-diethylaminocoumarin-3-carboxylic acid (DEAC) was purchased from Pharmachem International, and 5-carboxytetramethylrhodamine (TAMRA) was purchased from AnaSpec. All other reagents were purchased from Sigma-Aldrich. All reagents were used without further purification. Samples were photolyzed using an Oriel mercury arc lamp (200 W). A UV band-pass filter (UG-1) centered at 360 nm and Hg line filters (405 ± 10 nm and 546 ± 10 nm) were purchased from Newport.

Synthesis

Synthesis of Hydroxocobalamin Ethylenediamine (HOCbl-ethylenediamine)—

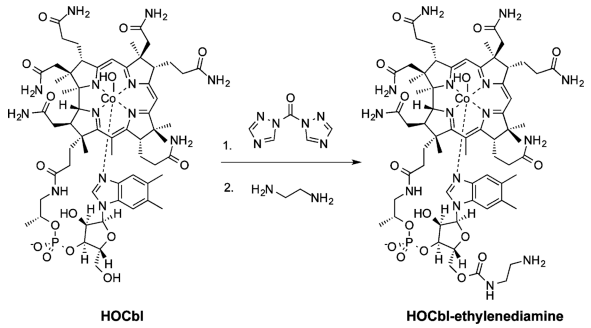

Hydroxocobalamin (**HO-Cbl**; 0.1034 g, 75 μmol) and 1,1′-carbonyldi-(1,2,4-triazole) (CDT; 0.2457 g, 820 μmol) were added to an oven-dried round-bottom flask. The vessel was purged with Ar. Dry DMF (3 mL) was added to the flask, and the mixture stirred at room temperature for 1 h. Ethylenediamine (0.4351 g, 720 μmol) was added to the reaction mixture, and stirring continued for another 18 h. The desired compound was purified by reverse phase flash chromatography (C-18 column) using a linear gradient binary solvent system (solvent A: 0.1% TFA/H_2O; solvent B: 0.l% TFA/CH_3CN) with a ratio of A:B that varied from 97:3 to 35:65 over 10 column volumes. Removal of solvent by lyophilization afforded a red solid (0.0673 g, 63%) (Figure S1). ESI MS [**HOCbl-ethylenediamine**, –OH]$^+$ calcd. for $C_{65}H_{94}N_{15}O_{15}PCo$: *m/z* = 1414.6123, found 1414.6030. [HOCbl-ethylenediamine, –OH, +H]$^{+2}$ calcd for $C_{65}H_{95}N_{15}O_{15}PCo$: *m/z* = 707.8101, found 707.8069. ^{1}H NMR (400 MHz, D_2O) δ = 7.12 (s, 1 H), 6.48 (s, 1 H), 6.42 (s, 1 H), 6.25 (s, 1 H), 6.18 (d, *J* = 3.0 Hz, 1 H), 4.57 (d, *J* = 12.0 Hz, 1 H), 4.30–4.21 (m, 3 H), 4.19 (t, *J* = 3.4 Hz, 1 H), 4.14–4.03 (m, 2 H), 3.59 (d, *J* = 14.4 Hz, 1 H), 3.53 (d, *J* = 10.9 Hz, 1 H), 3.43 (dd, *J* = 5.1, 11.1 Hz, 1 H), 3.27–3.15 (m, 4 H), 3.01–2.96 (m, 1 H), 2.95–2.86 (m, 1 H), 2.74 (d, *J* = 7.1 Hz, 2 H), 2.72–2.69 (m, 2 H), 2.66 (s, 6 H), 2.59 (s, 6 H), 2.57–2.47 (m, 1 H), 2.39 (s, 2 H), 2.24 (s, 3 H), 2.19 (s, 4 H), 2.16–1.98 (m, 5 H), 1.88 (d, *J* = 8.7 Hz, 7 H),

1.84–1.74 (m, 2 H), 1.45 (d, *J* = 7.1 Hz, 7 H), 1.35 (s, 4 H), 1.32 (s, 4 H), 1.30–1.29 (m, 1 H), 1.22 (d, *J* = 6.3 Hz, 4 H), 1.04–0.86 (m, 2 H), 0.48 (s, 3 H).

Synthesis of HOCbl-1:

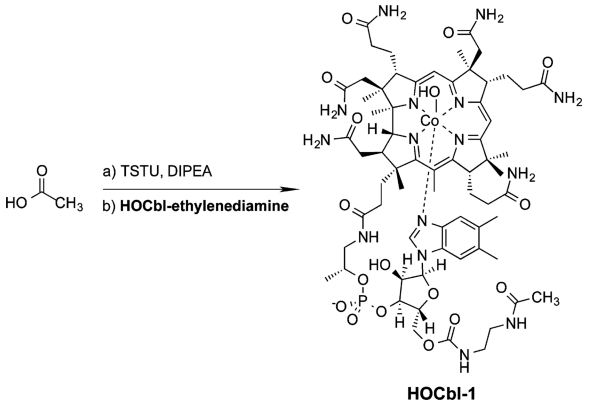

N,N,N′,N′-Tetramethyl-*O*-(*N*-succinimidyl)uranium tetrafluoroborate (TSTU, 0.0065 g, 22 μmol), acetic acid (0.0010 g, 18 μmol), and *N,N*-diisopropylethylamine (DIPEA, 0.0074 g, 57 μmol) were mixed for 2 h in a DMF:dioxane:water solution (2:2:1, 250 μL). **HOCbl-ethylenediamine** (0.0057 g, 4.0 μmol) was added and the reaction mixed for 18 h. The desired compound was purified by HPLC (semiprepative C-18 column) using a linear gradient binary solvent system (solvent A: 0.1% TFA/H_2O; solvent B: 0.1% TFA/CH_3CN) with a ratio of A:B that varied from 97:3 (0 min) to 10:90 (40 min). Removal of solvent by lyophilization afforded a red solid (0.0051 g, 88%) (Figure S2). ESI MS [HOCbl-1, –OH, $+H]^{+2}$ calcd. for $C_{67}H_{96}N_{15}O_{16}PCo$: *m/z* = 728.3115, found 728.2964. ^1H NMR (400 MHz, D_2O) δ = 7.12 (s, 1 H), 6.48 (s, 1 H), 6.42 (s, 1 H), 6.26–6.23 (m, 1 H), 6.18 (d, *J* = 2.9 Hz, 1 H), 4.57 (d, *J* = 12.0 Hz, 1 H), 4.31–4.21 (m, 3 H), 4.19 (t, *J* = 3.4 Hz, 1 H), 4.14–4.02 (m, 2 H), 3.59 (d, *J* = 14.3 Hz, 1 H), 3.53 (d, *J* = 10.8 Hz, 1 H), 3.43 (dd, *J* = 4.8, 11.1 Hz, 1 H), 3.27–3.16 (m, 4 H), 3.00–2.96 (m, 1 H), 2.90 (dd, *J* = 9.7, 14.4 Hz, 1 H), 2.74 (d, *J* = 7.2 Hz, 2 H), 2.72–2.69 (m, 2 H), 2.66 (s, 6 H), 2.59 (s, 5 H), 2.56 (d, *J* = 4.1 Hz, 1 H), 2.55–2.51 (m, 1 H), 2.39 (s, 2 H), 2.24 (s, 3 H), 2.19 (s, 4 H), 2.14 (br. s., 1 H), 2.13–2.01 (m, 4 H), 1.88 (d, *J* = 8.6 Hz, 7 H), 1.84–1.74 (m, 2 H), 1.45 (d, *J* = 7.0 Hz, 6 H), 1.32 (s, 4 H), 1.35 (s, 3 H), 1.31–1.28 (m, 1 H), 1.22 (d, *J* = 6.3 Hz, 4 H), 1.01–0.86 (m, 2 H), 0.48 (s, 3 H).

Synthesis of HOCbl-2:

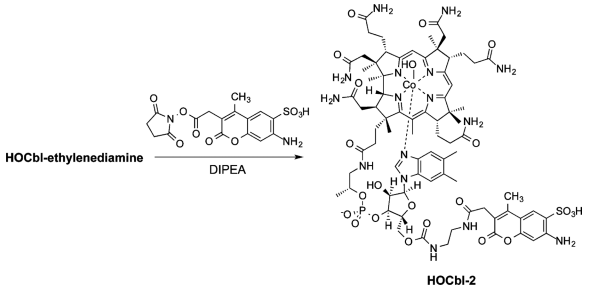

Alexa350 *N*-succinimidyl ester (0.0017 g, 4.1 μmol), **HOCbl-ethylenediamine** (0.0091 g, 6.4 μmol), and DIPEA (0.0030 g, 23 μmol) were mixed in DMF for 18 h. The desired

compound was purified by HPLC (semiprepative C-18 column) using a linear gradient binary solvent system (solvent A: 0.1% TFA/H_2O; solvent B: 0.1% TFA/CH_3CN) with a ratio of A:B that varied from 97:3 (0 min) to 10:90 (40 min). Removal of solvent by lyophilization afforded a red solid (0.0055 g, 78%) (Figure S3). ESI MS [HOCbl-2, –OH, +2H]$^{+2}$ calcd for $C_{77}H_{104}N_{16}O_{21}PSCo$: *m/z* = 855.3176, found 855.3137. ^{1}H NMR (400 MHz, D_2O) δ = 7.97 (s, 1 H), 7.09 (s, 1 H), 6.62 (s, 1 H), 6.46 (s, 1 H), 6.38 (s, 1 H), 6.17 (d, *J* = 3 Hz, 1 H), 6.15 (s, 1 H), 4.55 (d, *J* = 12.1 Hz, 1 H), 4.31–4.17 (m, 7 H), 4.09 (d, *J* = 7.7 Hz, 1 H), 3.97 (d, *J* = 10.4 Hz, 1 H), 3.58 (d, *J* = 14.0 Hz, 1 H), 3.53–3.48 (m, 1 H), 3.46 (d, *J* = 2.5 Hz, 2 H), 3.36 (dd, *J* = 5.5, 10.6 Hz, 1 H), 3.28–3.22 (m, 1 H), 3.17 (dd, *J* = 7.7, 15.2 Hz, 2 H), 3.02–2.85 (m, 2 H), 2.76–2.65 (m, 3 H), 2.65–2.48 (12 H) 2.38 (br. s., 2 H), 2.30–2.17 (m, 6 H), 2.13 (s, 3 H), 2.09–1.98 (m 2 H), 1.91–1.83 (m, 4 H), 1.82–1.70 (m, 1 H), 1.48–1.38 (m, 5 H), 1.37–1.26 (m, 5 H), 1.22 (d, *J* = 6.2 Hz, 3 H), 0.97–0.82 (m, 1 H), 0.47 (br. s., 3 H).

Synthesis of HOCbl-3:

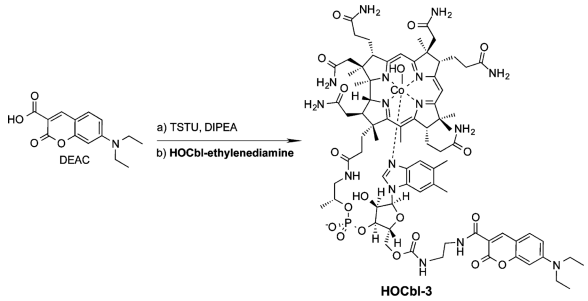

HOCbl-3 was synthesized and purified in the same manner as **HOCbl-1** using TSTU (0.0070 g, 23 μM), 7-(diethylamino)coumarin-3-carboxylic acid (0.0031 g, 12 μM), DIPEA (0.0052 g, 40 μmol), and **HOCbl-ethylenediamine** (0.0107 g, 75 μmol) to afford an orange solid (0.0086 g, 79%) (Figure S4). ESI MS [HOCbl-3, –OH, +H]$^{+2}$ calcd for $C_{79}H_{107}N_{16}O_{18}PCo$: *m/z* = 828.8510, found 828.8352. ^{1}H NMR (400 MHz, D_2O) δ = 8.25 (s, 1 H), 7.30 (d, *J* = 9.1 Hz, 1 H), 7.06 (s, 1 H), 6.66 (d, *J* = 9.1 Hz, 1 H), 6.43 (s, 1 H), 6.40 (s, 1 H), 6.28 (s, 1 H), 6.15 (s, 1 H), 6.11 (d, *J* = 2.6 Hz, 1 H), 4.49 (d, *J* = 10.8 Hz, 1 H), 4.26–4.14 (m, 4 H), 4.10–4.03 (m, 1 H), 3.68 (t, *J* = 5.9 Hz, 1 H), 3.56 (d, *J* = 14.4 Hz, 1 H), 3.50–3.34 (m, 6 H), 3.21 (t, *J* = 5.9 Hz, 1 H), 2.87 (dd, *J* = 9.5, 14.3 Hz, 1 H), 2.68 (d, *J* = 12.9 Hz, 4 H), 2.62–2.44 (m, 4 H), 2.35 (s, 2 H), 2.17 (s, 3 H), 2.11 (s, 3 H), 1.83 (s, 3 H), 1.39 (s, 2 H), 1.28 (t, *J* = 15.7 Hz, 6 H), 1.19 (d, *J* = 6.2 Hz, 2 H), 1.15–1.04 (m, 6 H), 0.40 (br. s., 3 H).

Synthesis of HOCbl-4:

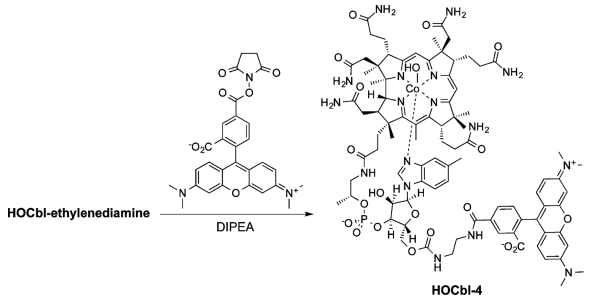

HOCbl-4 was synthesized and purified in the same manner as **HOCbl-2** using 5-carboxy-tetramethylrhodamine *N*-succinimidyl ester (0.0023 g, 43 μmol), **HOCbl-ethylenediamine** (0.0101 g, 7 μmol), and DIPEA (0.0056 g, 43 μM) to afford an orange solid (0.0062 g, 77%) (Figure S5). ESI MS $[HOCbl\text{-}4]^{+}$ calcd for $C_{90}H_{115}N_{17}O_{19}PCo$: m/z = 1827.7625, found 1827.7492. $[HOCbl\text{-}4, +H]^{+2}$ calcd for $C_{90}H_{116}N_{17}O_{19}PCo$: m/z = 914.3852, found 914.3815. ^{1}H NMR (400 MHz, D_2O) δ = 8.49 (s, 1 H), 8.09 (d, J = 7.7 Hz, 1 H), 7.50 (d, J = 7.9 Hz, 1 H), 7.13 (dd, J = 3.8, 9.5 Hz, 2 H), 7.08 (s, 1 H), 6.84 (d, J = 9.6 Hz, 2 H), 6.59 (s, 2 H), 6.48 (s, 1 H), 6.40 (s, 1 H), 6.21 (s, 2 H), 4.60–4.50 (m, 1 H), 4.31–4.16 (m, 6 H), 4.12 (d, J = 8.9 Hz, 2 H), 3.62–3.47 (m, 4 H), 3.42 (br. s., 3 H), 3.12 (s, 9 H), 2.75–2.49 (m, 14 H), 2.38 (s, 2 H), 2.21 (s, 4 H), 2.10 (s, 4 H), 2.07–1.97 (m, 4 H), 1.87 (s, 5 H), 1.42 (s, 8 H), 1.30 (d, J = 3.0 Hz, 8 H), 1.16 (d, J = 6.2 Hz, 5 H), 0.91 (d, J = 11.3 Hz, 2 H), 0.46 (br. s., 3 H).

Synthesis of N-Acetylcysteinyl Cbl (NAcSCbl), Ribose 5′-OH Acetylated N-Acetylcysteinyl Cbl (NAcSCbl-1), and N-Acetylcysteinyl Cbl-Fluorophore Conjugates (NAcSCbl-2, NAcSCbl-3, and NAcSCbl-4)—NAcSCbls were synthesized using a procedure modified from the literature.[19,31] To an acetate buffered (185 μL, 100 mM, pH 5.5) solution of **HOCbl** (10 mg, 7.38 μmol, 1 equiv) was added 48 μL of *N*-acetylcysteine (**NAcSH**) solution (200 mM, 9.59 μmol, 1.3 equiv). The product was precipitated in cold acetone (2.5 mL, 10 volumes) and triturated with cold acetone (3×). The dark red precipitate was redissolved in 500 μL of acetate buffer, and the purity and yield were checked by LC-MS and absorbance (Figure S6).

NAcSCbl:

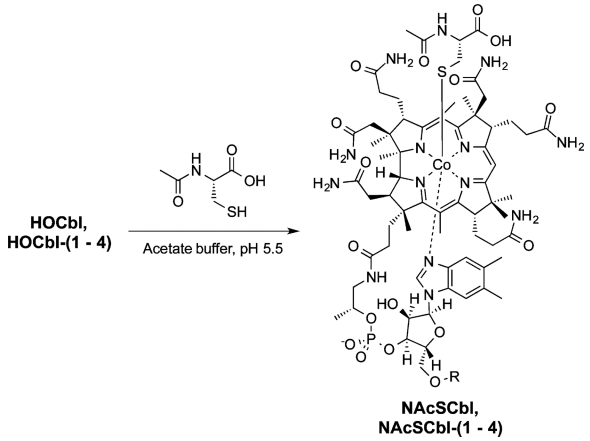

Dark red solid, yield (57%) and purity (97%). ESI MS [NAcSCbl, –H, +3Na]$^{2+}$ calcd. for $C_{67}H_{95}N_{14}O_{17}PSCoNa_3$ *m/z* = 779.2742, found 779.2827. ^{1}H NMR (400 MHz, D_2O) δ = 7.19 (br. s., 1 H), 6.91 (br. s., 1 H), 6.37 (br. s., 1 H), 6.26 (d, *J* = 6.26 Hz, 1 H), 6.05 (s, 1 H), 4.59 (t, *J* = 5.5 Hz, 1 H), 4.53 (d, *J* = 9.4 Hz, 1 H), 4.32–4.16 (m, 3 H), 4.06 (d, *J* = 8.4 Hz, 1 H), 4.02–3.93 (m, 2 H), 3.86 (d, *J* = 12.7 Hz, 1 H), 3.71 (dd, *J* = 13 Hz, 3.6 Hz, 1 H), 3.55 (br. s., 1 H), 3.37–3.24 (m, 3 H), 3.05–2.88 (m, 5 H), 2.84–2.65 (m, 4 H), 2.64–2.45 (m, 11 H), 2.44–2.28 (m, 7 H), 2.20 (br. s., 7 H), 2.09–2.01 (m, 7 H), 1.96 (br. s., 2 H), 1.87 (s, 3 H), 1.81 (s, 3 H), 1.76 (m, 1 H), 1.37 (br. s., 10 H), 1.27 (br. s., 2 H), 1.23–1.18 (m, 1 H), 1.06–0.83 (m, 1 H), 0.38 (br. s., 2 H).

Ribose 5′-OH Acetylated N-Acetylcysteinyl Cbl (NAcSCbl-1)—Red solid, yield (85%) and purity (98%) (Figure S7). ESI MS [NAcSCbl-1, +Na]$^+$ calcd. for $C_{72}H_{104}N_{16}O_{19}PSCoNa$: *m/z* = 1641.6352, found 1641.6921. [NAcSCbl-1, +2Na]$^{+2}$ calcd. for $C_{72}H_{104}N_{16}O_{19}PSCoNa_2$: *m/z* = 832.3125, found 832.3166. [NAcSCbl-1, –H, +3Na]$^{+2}$ calcd. for $C_{72}H_{103}N_{16}O_{19}PSCoNa_3$: *m/z* = 843.30355, found 843.30982. ^{1}H NMR (400 MHz, D_2O) δ = 7.13 (s, 1 H), 6.9 (s, 1 H), 6.33 (s, 1 H), 6.19 (d, 1 H), 6.01 (s, 1 H), 4.56–4.45 (m, 2 H), 4.30–4.20 (m, 2 H), 4.20–4.10 (m, 2 H), 4.07 (dd, *J* = 12.5 Hz, *J* = 2.3 Hz, 1 H), 4.01 (d, *J* = 9.8 Hz, 1 H), 3.9 (t, *J* = 6.7 Hz, 1 H), 3.51 (d, *J* = 14.1 Hz, 1 H), 3.27 (d, *J* = 10.6 Hz, 1 H), 3.23–3.14 (m, 4 H), 3.04–2.94 (m, 1 H), 2.75–2.64 (m, 3 H), 2.63–2.46 (m, 6 H), 2.44 (s, 3 H), 2.39 (s, 2 H), 2.37–2.27 (m, 2 H), 2.22 (s, 3 H), 2.15 (s, 4 H), 2.08 (d, *J* = 13.3 Hz, 2 H), 1.99 (m, 1 H), 1.87–1.81 (m, 6 H), 1.78–1.71 (m, 5 H), 1.45–1.37 (m, 2 H), 1.35 (s, 6 H), 1.31 (s, 4 H), 1.23 (s, 3 H), 1.16 (d, *J* = 6.3 Hz, 3 H), 0.99–0.81 (m, 2 H), 0.36 (br. s., 3 H).

N-Acetylcysteinylcobalamin-AlexaFluor350 Conjugate (NAcSCbl-2)—Red solid, yield (81%) and purity (92%) (Figure S8). ESI MS [NAcSCbl-2, –H, +2Na]$^+$ calcd. for $C_{82}H_{109}N_{17}O_{24}PS_2CoNa_2$: *m/z* = 1915.6138, found 1915.6365. [NAcSCbl-2, –H, +3Na]$^{+2}$ calcd. for $C_{82}H_{109}N_{17}O_{24}PS_2CoNa_3$: *m/z* = 969.3018, found 969.3753. ^{1}H NMR (400 MHz, D_2O) δ = 7.89 (s, 1 H), 7.13 (br. s., 1 H), 7.05 (s, 1 H), 6.88–6.70 (m, 2 H), 6.14 (d, *J* = 5.1 Hz, 1 H), 5.95 (s, 1 H), 4.53–4.48 (m, 1 H), 4.43 (br. s., 1 H), 4.12 (dd, *J* = 9.6, 17.8 Hz, 2 H), 3.96 (d, *J* = 9.0 Hz, 1 H), 3.88 (d, *J* = 10.6 Hz, 1 H), 3.80–3.73 (m, 1 H), 3.70–3.63 (m, 1 H), 3.53–3.47 (m, 1 H), 3.22–2.96 (m, 3 H), 2.95–2.75 (m, 2 H), 2.64–2.46 (m, 3 H), 2.43–2.21 (m, 5 H), 2.17–1.89 (m, 8 H), 1.84–1.34 (m, 13 H), 1.33–1.15 (m, 7 H), 1.13–0.85 (m, 4 H), 0.47–0.16 (m, 2 H).

N-Acetylcysteinyl Cbl-Diethylaminocoumarin Conjugate (NAcSCbl-3)—Orange solid, yield (74%) and purity (96%) (Figure S9). ESI MS [NAcSCbl-3, –H, +3Na]$^{+2}$ calcd. for $C_{84}H_{114}N_{17}O_{21}PSCoNa_3$: *m/z* = 943.8430, found 943.8364. ^{1}H NMR (400 MHz, D_2O) δ = 8.28 (s, 1 H), 7.32 (br. s., 1 H), 7.07 (s, 1 H), 6.84 (d, *J* = 9.2 Hz, 1 H), 6.73–6.60 (m, 1 H), 6.44–6.24 (m, 2 H), 6.17–6.08 (m, 1 H), 5.81 (br. s., 1 H), 4.49 (br. s., 1 H), 4.35–4.20 (m, 2 H), 4.12 (d, *J* = 10.6 Hz, 1 H), 4.04 (d, *J* = 9.0 Hz, 1 H), 3.91 (br. s., 1 H), 3.70 (t, *J* = 5.7 Hz, 1 H), 3.59–3.41 (m, 4 H), 3.41–3.26 (m, 4 H), 3.26–3.18 (m, 1 H), 2.79–2.60 (m, 3 H), 2.58–2.26 (m, 10 H), 2.19–2.09 (m., 4 H), 2.08–2.01 (m, 2 H), 1.99–1.89 (m, 2 H), 1.85 (s, 3 H), 1.77 (br. s., 2 H), 1.45–1.29 (m, 5 H), 1.28–1.02 (m, 11 H), 0.40 (s, 2 H).

N-Acetylcysteinyl Cbl-TAMRA Conjugate (NAcSCbl-4)—Pink solid, yield (66%) and purity (98%) (Figure S10). ESI MS $[NAcSCbl\text{-}4]^{+}$ calcd for $C_{95}H_{123}N_{18}O_{22}PSCo$: *m/z* = 1989.7850, found 1989.7780. $[NAcSCbl\text{-}4, +H]^{+2}$ calcd for $C_{90}H_{124}N_{18}O_{22}PSCo$: *m/z* = 995.3664, found 995.3922. $[NAcSCbl\text{-}4, +Na]^{+2}$ calcd for $C_{95}H_{123}N_{18}O_{22}PSCoNa$: *m/z* = 1006.3874, found 1006.3831. $[NAcSCbl\text{-}4, –H, +2Na]^{+2}$ calcd for $C_{95}H_{122}N_{18}O_{22}PSCoNa_2$: *m/z* = 1017.3784, found 1017.3744. ^1H NMR (400 MHz, D_2O) δ = 8.52 (d, *J* = 9.4 Hz, 1 H), 8.09 (br. s., 1 H), 7.55–7.37 (m, 2 H), 7.17–6.95 (m, 4 H), 6.82–6.75 (br. s., 2 H), 6.41 (br. s., 2 H), 6.35 (br. s., 1 H), 6.24 (br. s., 1 H), 4.48 (d, *J* = 9.5 Hz, 1 H), 4.35–4.14 (m, 3 H), 4.06 (br. s., 1 H), 3.90 (br. s., 1 H), 3.75–3.68 (m, 1 H), 3.65–3.52 (m, 2 H), 3.51–3.36 (m, 3 H), 3.33–3.27 (m, 1 H), 3.26 (d, *J* = 5.3 Hz, 1 H), 3.22–3.19 (m, 2 H), 3.15 (d, *J* = 6.0 Hz, 2 H), 3.04 (br. s., 13 H), 3.01–2.93 (m, 2 H), 2.71–2.59 (m, 3 H), 2.58–2.26 (m, 12 H), 2.24–1.98 (m, 10 H), 1.89–1.71 (m, 6 H), 1.45–1.21 (m, 9 H), 1.21–1.07 (m, 5 H).

LC-MS ESI Analysis of NAcSCbl and Photolysis Products

NAcSCbl and derivatives **1–4** (40 μM, 100 μL) and photolyzed samples (20 μM, 100 μL) were initially analyzed using an Agilent 1200 series LC-MS equipped with a reverse phase C_{18} column scanning in positive ion mode (Figures S11–S15). Samples were eluted using a binary gradient solvent system (A: 0.1% v/v acetic acid/H_2O; B: 100% CH_3CN) with a ratio of A:B varying from 95:5 (0–4 min) to 1:9 (5–18 min) and then held constant (18–20 min). Elution was detected at 280 and 540 nm. Purity of the complexes was determined using the area under the curve of the 540 nm absorption since all starting materials and products share the same extinction coefficient at this wavelength. For full product characterization, purified **HOCbl** and **NAcSCbl** synthesis products were dissolved in MeOH (25 μM) and injected via electrospray ionization onto a high-resolution Thermo LTQ-FT-ICR-MS (<1.2 ppm) scanning in positive ion mode. For ^1H NMR analysis, the precipitates of **NAcSCbl** derivatives **1–4** were washed for a final time with deuterated acetone and then dried overnight before being scanned with a 400 MHz Varian NMR.

Photolytic Rate and Quantum Yield Estimation

Samples of **NAcSCbl, NAcSCbl-(1–4)**, and **MeCbl** (20 μM, 1 mL, 100 mM acetate buffer, pH 5.5) were placed in a room temperature water bath and photolyzed with a Thermo Oriel Hg Arc lamp equipped with a UV band-pass filter (UG-1, 360 nm) and Hg line filters (405 ± 10 nm and 546 ± 10 nm). Samples were scanned between 300 and 600 nm on a PerkinElmer Lambda 2 UV/vis spectrophotometer for changes in the absorption spectra. The amount of **HOCbl-(1–4)** in solution was determined by

$$[\mathbf{HOCbl}(\mathrm{M})]=(\Delta A_\lambda/\Delta\varepsilon_\lambda) \quad (1)$$

where ΔA_λ and $\Delta\varepsilon_\lambda$ are the change in the absorbance and extinction coefficient (M^{-1} cm^{-1}), respectively, at a given wavelength. The relative rate of photolysis was estimated from the initial slope of the [**HOCbl**] versus time and the ln[**HOCbl**] versus time (*n* = 3). The slope of the ln[**HOCbl**] vs time (*t*) provided a relative rate constant for the reaction ($k_{app\text{-}NAcSCbl}$) (Figures S16–S23). **MeCbl** served as a normalizing chemical actinometer, since its ε and Φ

have been reported throughout its absorption spectra (Figures S24–S26).[3] Since the solution was dilute and sensitive to changes in absorption with time, the rate of **MeCbl** photolysis at 360 nm was normalized to an apparent constant (k_{app}) of 1 and the samples' quantum yields ($\Phi_{NAcSCbl}$) at a given wavelength were determined by[32]

$$\frac{\frac{k_{NAcSCbl}}{k_{MeCbl}} * \varepsilon\Phi_{MeCbl}}{\varepsilon_{NAcSCbl}} = \Phi_{NAcSCbl} \quad (2)$$

where k is the photolysis rate of **NAcSCbl-(1–4)** normalized to the photolysis rate of **MeCbl**, $\varepsilon_{NAcSCbl}$ is the extinction coefficient of **NAcSCbl-(1–4)** at a given wavelength, and $\varepsilon\Phi_{MeCbl}$ is the product efficiency of **MeCbl** photolysis.[32]

Thiyl Radical Detection by Electron Paramagnetic Resonance (EPR)

Immediately after photolysis or addition of peroxide (*vide infra*), steady-state EPR spectroscopy was conducted using a JEOL FA-100 spectrometer operating at X-band (9.5 GHz) with 100 kHz field modulation. Samples were contained in 0.5 mm ID (1.0 mm OD) quartz capillaries and inserted into the center of the TE_{011} cylindrical resonator of the spectrometer. Spectra were collected over 4 min at a center field of 3362 G, a sweep width of 80 G, a field modulation of 0.8 G, and microwave power of 1 mW. Computer simulation was used to determine the g factors and electron–nuclear hyperfine interactions. *(1) Light-triggered cobalamin-derived thiyl radicals*. Solutions of either **NAcSCbl** or **NAcSCbl-4** (1 mM, 100 uL) were mixed with phenyl *t*-butyl nitrone (PBN, 100 mM) in acetate buffer (100 mM, pH 5.5) and then purged with N_2 for 10 min. Samples were loaded into a quartz capillary (0.5 mm ID, 1.0 mm OD) and then left in the dark or photolyzed (546 ± 10 nm) using a Hg arc lamp for 10 min. The samples were immediately scanned as the thiol-PBN adduct signal decayed with increasing post illumination time. *(2) Peroxidase generated thiyl radicals*. **NAcSH** radicals were generated from horseradish peroxidase catalyzed oxidation according to a literature procedure.[33] Briefly, **NAcSH** (5 mM), PBN (100 mM), *p*-phentidine (500 μM), and horseradish peroxidase (2 μg/mL, ~2 units/mL) were mixed in phosphate buffered saline (100 μL, 100 mM, 1 mM EDTA, pH 8.0) and then purged with N_2 for 10 min. Hydrogen peroxide (250 μM) was quickly added to initiate oxidation, and the solution was loaded into a quartz capillary and scanned immediately since the thiol-PBN adduct signal decays with time.

RESULTS AND DISCUSSION

Previous work has demonstrated that *N*-acetyl-L-cysteine (**NAcSH**) forms stable thiolato adducts with Cbl.[31] Therefore, we employed **NAcSH** as our model mercaptan and prepared a variety **NAcSCbl** derivatives (Scheme 1). The ribose 5′-hydroxyl moiety of **HOCbl** was activated using 1,1′-carbonyl-ditriazole (CDT) and then subsequently exposed to ethylenediamine to furnish **HOCbl-ethylenediamine**. The latter provides an amine handle upon which light-capturing antennas in the form of fluorophores will be installed (*vide infra*). The thiolato-Cbl derivatives were subsequently prepared under mildly acidic reaction conditions, which enables the cysteine thiolate to displace Co^{III}-bound H_2O via β ligand

exchange to generate the desired Co^{III}–S bond. Successful thiolato-Cbl formation is signaled by a change in the visible absorption spectrum (Figure 1) and LC-MS analysis. **HOCbl** displays an absorbance spectrum with one sharp transition arising at 350 nm (γ band) and a broad visible absorption centered on 525 nm (α/β band). **HOCbl** conversion to thiolato derivatives produces a noticeable color change in solution from red to purple, with maxima at 334, 370, and 535 nm.[22,23,31] The similarities between the **NAcSCbl** and the **MeCbl** in the UV range are consistent with the notion that both thiolato and alkyl ligands have comparable donor character and electronic transitions.

We monitored the changes in the absorption spectrum of **NAcSCbl** (20 μM, 100 mM acetate buffer, pH 5.5) during photolysis to assess the extent of unreacted **NAcSCbl** as a function of time (Figures 2, 3, S16–S17).[3] **NAcSCbl** photolysis at 360 ± 10 nm produced significant spectral changes with isosbestic points at 340, 365, 404, 418, 446, and 540 nm. In agreement with previous studies, the photoproduct spectrum resembled **HOCbl**, which was confirmed by LC-MS analysis (Figures 1, 2, S11).[19–21] Illumination of **NAcSCbl** at 360 ± 10 nm induces the formation of **HOCbl** at a rate approximately 3 orders of magnitude slower than **MeCbl** (Table 1, Figures 3, S16, S17). As expected, **NAcSCbl** samples stored in the dark display insignificant decomposition compared to the irradiated samples (Figure S17).

We also investigated the photolysis of NAcSCbl using blue (405 ± 10 nm) and green (546 ± 10 nm) light by determining the propensity for photolysis measured as Φ (photolysis product formed per photons absorbed). The relative photolysis Φ of **NAcSCbl** under the three illumination conditions was determined by comparing the photolysis rates of **NAcSCbl** with those of **MeCbl**, since the Φ for the latter at all three wavelengths have been previously reported (Table 1, Figures S17–S19, S24–S26).[3] The rates of photolysis were normalized using the **MeCbl** photolysis rate at 360 nm as a baseline, and the quantum yield was determined from the ratio of these rates using eq 2. For all the wavelengths tested, the Φ for **NAcSCbl** are several orders of magnitude lower than those for **MeCbl**, indicating that the former are significantly less prone to photolysis than the latter. These lower Φ are responsible for the greatly reduced rate of **NAcSCbl** photolysis since the ε for both **MeCbl** and **NAcSCbl** are nearly identical at each wavelength tested. In addition, **NAcSCbl** displays a decreasing Φ with increasing wavelength with the Φ at 546 nm an order of magnitude lower than at 360 nm. This trend stands in stark contrast to most alkylCbls whose Φ remain relatively constant (20–30%) throughout their absorption spectra.[3,14] The dramatic reduction in both Φ and rate of thiolato-Cbls photolysis relative to alkylCbls is intriguing, especially given the similarities in Co–ligand bonding interactions in both species that have been noted by others.[22,23] Moreover, theoretical analyses of Co–C and Co–S bonding suggest that the latter may in fact be weaker with homolytic dissociation energies estimated at 26 kcal/mol for glutathionyl-Cbl and 37 kcal/mol for **MeCbl**.[1,5–9,23] A possible explanation for the comparatively modest photoresponsiveness of thiolato-Cbls may be a reduced diffusivity from the solvent caged radical pair of the heavier cysteine thiyl radical, leading to greater geminate recombination. Indeed, the observed photolysis Φ of alkylCbls arise from competition between separation of the alkyl and Co^{II} radical pair versus recombination to an intact complex. Larger alkyl ligands produce a greater fraction of recombination than their smaller counterparts.[1,14] In addition, crystal structures of model thiolato-Cbls reveal

favorable noncovalent bonding interactions between the **NAcSH** ligand and the Cbl nucleus, which could improve the overall stability of the complex.[21,34–36] Both of these structural features could lead to greater thiyl-Co^{II} radical recombination and a concurrent reduction in the apparent Φ. Indeed, radical recombination within a solvent cage versus escape dictates the apparent Φ for alkylCbls.[1,2,10,13,37,38]

We have previously demonstrated that alkylCbls with appended fluorophores suffer enhanced photolysis rates at wavelengths absorbed by the fluorophore.[30] We were interested in whether this approach could modulate the rate of photolysis for thiolato-Cbls as well. Therefore, we attached Alexa350 (λ_{max} = 350 nm), 7-(diethylamino)-coumarin-3-carboxylic acid (DEAC, λ_{max} = 423 nm), and 5-carboxytetramethylrhodamine (TAMRA, λ_{max} = 555 nm) to the free amine of **HOCbl-ethylenediamine** and subsequently generated the corresponding thiolato-Cbls (Scheme 1, Chart 1): **NAcSCbl-2, NAcSCbl-3**, and **NAcSCbl-4**, respectively. We also prepared a control compound, in which the fluorophore in **NAcSCbl-(2–4)** is replaced with an acetyl moiety (**NAcSCbl-1**). The fluorophores employed in derivatives **NAcSCbl-(2–4)** were chosen to overlap with and thereby increase the ε of the three primary Cbl absorption bands.

UV/vis absorption spectroscopy was used to assess the rate of photolysis of **NAcSCbl** derivatives **1–4**, and homolysis was confirmed by LC-MS. Not surprisingly, the Φ and relative reaction rate for the photolysis (360 nm) of the mono-acetylated derivative **NAcSCbl-1** [$k_{app} = (1.6 \pm 0.2) \times 10^{-3}$; $\Phi = (4.2 \pm 0.5) \times 10^{-4}$] and its nonacetylated counterpart **NAcSCbl** [$k_{app} = (1.6 \pm 0.3) \times 10^{-3}$; $\Phi = (4.4 \pm 0.8) \times 10^{-4}$] are virtually identical (Tables 1 and S1, Figure S20). The relative rate of 360 nm induced photolysis of the Alexa350 derivative, **NAcSCbl-2**, is nearly twice as large as the corresponding rates for **NAcSCbl** and **NAcSCbl-1** (Table 2, Figures 2, S20, S21, S27). This rate increase tracks with a corresponding increase in the extinction coefficient of **NAcSCbl-2**, implying that the rate change is due to increased photon absorption by the complex. In an analogous vein, DEAC modified **NAcSCbl-3** [$k_{app} = (1.1 \pm 0.1) \times 10^{-4}$; $\Phi = (1.1 \pm 0.1) \times 10^{-4}$] undergoes photolysis at 405 ± 10 nm, an order of magnitude more rapidly than **NAcSCbl** [$k_{app} = (1.1 \pm 0.1) \times 10^{-5}$; $\Phi = (1.3 \pm 0.1) \times 10^{-4}$] (Table 2, Figures S22, S28). The Φ for both complexes are nearly identical. However, the ε for **NAcSCbl-3** is an order of magnitude larger than that for **NAcSCbl**. Finally, **NAcSCbl-4** displays an analogous trend for photolysis at 546 nm. The relative photolytic rate of **NAcSCbl-4** is an order of magnitude greater than **NAcSCbl** in spite of the fact that the Φ for both complexes are nearly the same [$\Phi_{NAcSCbl} = (1.5 \pm 0.1) \times 10^{-5}$ versus $\Phi_{NAcSCbl\text{-}4} = (0.92 \pm 0.05) \times 10^{-5}$]. Once again, the primary driving force for the relative rates is the significantly greater photon capturing ability of **NAcSCbl-4** at 546 nm ($\varepsilon_{NAcSCbl} = 6400\ M^{-1}\ cm^{-1}$ versus $\varepsilon_{NAcSCbl\text{-}4} = 84\,000\ M^{-1}\ cm^{-1}$) (Table 2, Figures S23, S29). Relative to alkylCbls, the Φ of thiolato-Cbls are low. However, the photolytic efficiencies (Φε) exhibited by the fluorophore modified Cbls display comparable ligand release values to some similar, visible light responsive caging groups.[39–42] Moreover, reduced photolability may provide an advantage since the simple act of imaging via fluorescent microscopy induces rapid photocleavage of the extremely susceptible alkylCbls. Finally, these results demonstrate that fluorophores can act as photon antennas, offering the means to modulate the rate of thiolato-Cbl photolysis.[30]

We have assessed the photolytic fate of the *N*-acetylcysteine ligand by EPR. As noted above, previous reports have postulated that thiolato-Cbls undergo decomposition to generate a Co^{II} and thiyl radical species.[20,22,43] However, to the best of our knowledge, the direct observation of a thiyl radical adduct has not been experimentally demonstrated. Both **NAcSCbl** and **NAcSCbl-4** (1 mM, 100 mM acetate buffer, pH 5.5) were separately photolyzed in the presence of the radical trap PBN (100 μM) and then analyzed by EPR spectroscopy (Figure 4, Scheme S1). Predictably, in the dark, neither complex produced a signal from paramagnetic species trapping (Figure 4a). However, upon illumination at 546 ± 10 nm, the expected triplet of doublets splitting was observed for both compounds with identical hyperfine couplings (Figure 4b,c; a^N = 16.2 G, a^H = 3.8 G). For comparison purposes, we generated and trapped an *N*-acetylcysteine thiyl radical produced by horseradish peroxidase catalyzed oxidation (100 mM TRIS buffer, 1 mM EDTA, pH ~ 8.0).[33] This procedure furnishes a thiyl radical with very similar hyperfines (Figure 4d, a^N = 15.7 G, a^H = 3.8 G). A small variation in a^N arises in the enzyme generated thiyl, but this effect likely arises from the difference in buffer pH and ionic strength required for peroxidase activity.[44] As a side note, we found that the EPR signal decays rapidly with time, and thus, the samples used in this study were quickly scanned after photolysis to ensure maximum signal intensity before decay.

CONCLUSIONS

We have demonstrated that thiolato-Cbls undergo ready photolysis at wavelengths throughout their absorption spectrum. Although the efficiency of thiolato-Cbl photolysis is significantly lower than that displayed by alkylCbls, the photoresponsiveness of thiolato-Cbls is comparable to that of many common caging groups.[39–42] Photolysis of thiolato-Cbls is more rapid with UV illumination than with visible light. However, we have demonstrated that fluorophores attached to the Cbl can enhance the photolytic rate at visible wavelengths. Finally, we have shown, for the first time, that a thiyl radical is generated upon photolysis of a thiolato-Cbl. The unique photochemistry of thiolato-Cbl suggests applications that range from light-induced peptide[45] and drug delivery[46] to photoinduced thiolene click reactions.[47,48]

Supplementary Material

Refer to Web version on PubMed Central for supplementary material.

Acknowledgments

We thank the National Institutes of Health (R01 CA79954) for financial support.

REFERENCES

1. Brown KL. Chem. Rev. 2005; 105:2075–2149. [PubMed: 15941210]
2. Banerjee, R., editor. Chemistry and Biochemistry of B_{12}. New York: Wiley; 1999.
3. Taylor RT, Smucker L, Hanna ML, Gill J. Arch. Biochem. Biophys. 1973; 156:521–533. [PubMed: 4718782]
4. Hogenkamp HPC. Biochemistry. 1966; 5:417–422. [PubMed: 5940929]
5. Qu Z, Hansen A, Grimme S. J. Chem. Theory Comput. 2015; 11:1037–1045. [PubMed: 26579755]

6. Hung RR, Grabowski JJJ. J. Am. Chem. Soc. 1999; 121:1359–1364.
7. Martin BD, Finke RG. J. Am. Chem. Soc. 1992; 114:585–592. [PubMed: 20000783]
8. Kozlowski PM, Kumar M, Piecuch P, Li W, Bauman NP, Hansen JA, Lodowski P, Jaworska M. J. Chem. Theory Comput. 2012; 8:1870–1894. [PubMed: 26593822]
9. Kobylianskii IJ, Widner FJ, Kraeutler B, Chen P. J. Am. Chem. Soc. 2013; 135:13648–13651. [PubMed: 24007238]
10. Sension RJ, Harris DA, Cole AG. J. Phys. Chem. B. 2005; 109:21954–21962. [PubMed: 16853853]
11. Lodowski P, Jaworska M, Andruniów T, Kumar M, Kozlowski PM. J. Phys. Chem. B. 2009; 113:6898–6909. [PubMed: 19374399]
12. Rury AS, Wiley TE, Sension RJ. Acc. Chem. Res. 2015; 48:860–867. [PubMed: 25741574]
13. Harris DA, Stickrath AB, Carroll EC, Sension RJ. J. Am. Chem. Soc. 2007; 129:7578–7585. [PubMed: 17530754]
14. Cole AG, Yoder LM, Shiang JJ, Anderson NA, Walker LA, Banaszak Holl MM, Sension RJ. J. Am. Chem. Soc. 2002; 124:434–441. [PubMed: 11792214]
15. Lodowski P, Jaworska M, Andruniów T, Garabato BD, Kozlowski PM. J. Phys. Chem. A. 2014; 118:11718–11734. [PubMed: 25383645]
16. Lodowski P, Jaworska M, Garabato BD, Kozlowski PM. J. Phys. Chem. A. 2015; 119:3913–3928. [PubMed: 25837554]
17. Wagner F, Bernhauer K. Ann. N. Y. Acad. Sci. 1964; 112:580–589. [PubMed: 14167291]
18. Adler N, Medwick T, Poznanski TJ. J. Am. Chem. Soc. 1966; 88:5018–5020.
19. Dolphin D, Johnson AW. J. Chem. Soc. 1965; 65:2174–2181. [PubMed: 14288329]
20. Tahara K, Matsuzaki A, Masuko T, Kikuchi J, Hisaeda Y. Dalt. Trans. 2013; 42:6410.
21. Suto RK, Brasch NE, Anderson OP, Finke RG. Inorg. Chem. 2001; 40:2686–2692. [PubMed: 11375680]
22. Conrad KS, Brunold TC. Inorg. Chem. 2011; 50:8755–8766. [PubMed: 21859072]
23. Eisenberg AS, Likhtina IV, Znamenskiy VS, Birke RL. J. Phys. Chem. A. 2012; 116:6851–6869. [PubMed: 22568547]
24. Shell TA, Lawrence DS. Acc. Chem. Res. 2015; 48:2866–2874. [PubMed: 26479305]
25. Smith WJ, Oien NP, Hughes RM, Marvin CM, Rodgers ZL, Lee J, Lawrence DS. Angew. Chem., Int. Ed. 2014; 53:10945–10948.
26. Rodgers ZL, Hughes RM, Doherty LM, Shell JR, Molesky BP, Brugh AM, Forbes MDE, Moran AM, Lawrence DS. J. Am. Chem. Soc. 2015; 137:3372–3378. [PubMed: 25697508]
27. Shell TA, Lawrence DS. J. Am. Chem. Soc. 2011; 133:2148–2150. [PubMed: 21275391]
28. Zelder F. Chem. Commun. 2015; 51:14004–14017.
29. Priestman MA, Shell TA, Sun L, Lee H-M, Lawrence DS. Angew. Chem., Int. Ed. 2012; 51:7684–7687.
30. Shell TA, Shell JR, Rodgers ZL, Lawrence DS. Angew. Chem., Int. Ed. 2014; 53:875–878.
31. Suarez-Moreira E, Hannibal L, Smith CA, Chavez RA, Jacobsen DW, Brasch NE. Dalton Trans. 2006:5269–5277. [PubMed: 17088966]
32. Challis JK, Hanson ML, Friesen KJ, Wong CS. Environ. Sci. Process. Impacts. 2014; 16:672. [PubMed: 24643336]
33. Ross D, Norbeck K, Moldeus P. J. Biol. Chem. 1985; 260:15028–15032. [PubMed: 2999101]
34. Randaccio L, Geremia S, Nardin G, Šlouf M, Srnova I. Inorg. Chem. 1999; 38:4087–4092.
35. Mukherjee R, McCaddon A, Smith CA, Brasch NE. Inorg. Chem. 2009; 48:9526–9534. [PubMed: 19780623]
36. Hannibal L, Smith CA, Jacobsen DW. Inorg. Chem. 2010; 49:9921–9927. [PubMed: 20863098]
37. Peng J, Tang K, McLoughlin K, Yang Y, Forgach D, Sension RJ. J. Phys. Chem. B. 2010; 114:12398–12405. [PubMed: 20815360]
38. Walker, La; Jarrett, JT.; Anderson, Na; Pullen, SH.; Matthews, RG.; Sension, RJ. J. Am. Chem. Soc. 1998; 120:3597–3603.

39. Klán P, Šolomek T, Bochet CG, Blanc A, Givens R, Rubina M, Popik V, Kostikov A, Wirz J. Chem. Rev. 2013; 113:119–191. [PubMed: 23256727]
40. Zayat L, Salierno M, Etchenique R. Inorg. Chem. 2006; 45:1728–1731. [PubMed: 16471986]
41. Umeda N, Takahashi H, Kamiya M, Ueno T, Komatsu T, Terai T, Hanaoka K, Nagano T, Urano Y. ACS Chem. Biol. 2014; 9:2242–2246. [PubMed: 25140990]
42. Haas KL, Franz KJ. Chem. Rev. 2009; 109:4921–4960. [PubMed: 19715312]
43. Brasch NE, Hsu T-LC, Doll KM, Finke RG. J. Inorg. Biochem. 1999; 76:197–209. [PubMed: 10605837]
44. Saracino GAA, Tedeschi A, D'Errico G, Improta R, Franco L, Ruzzi M, Corvaia C, Barone V. J. Phys. Chem. A. 2002; 106:10700–10706.
45. Lee H-M, Larson DR, Lawrence DS. ACS Chem. Biol. 2009; 4:409–427. [PubMed: 19298086]
46. Carling C-J, Viger ML, Nguyen Huu VA, Garcia AV, Almutairi A. Chem. Sci. 2015; 6:335–341. [PubMed: 25598962]
47. Hoyle CE, Bowman CN. Angew. Chem., Int. Ed. 2010; 49:1540–1573.
48. Lowe AB. Polym. Chem. 2014; 5:4820.

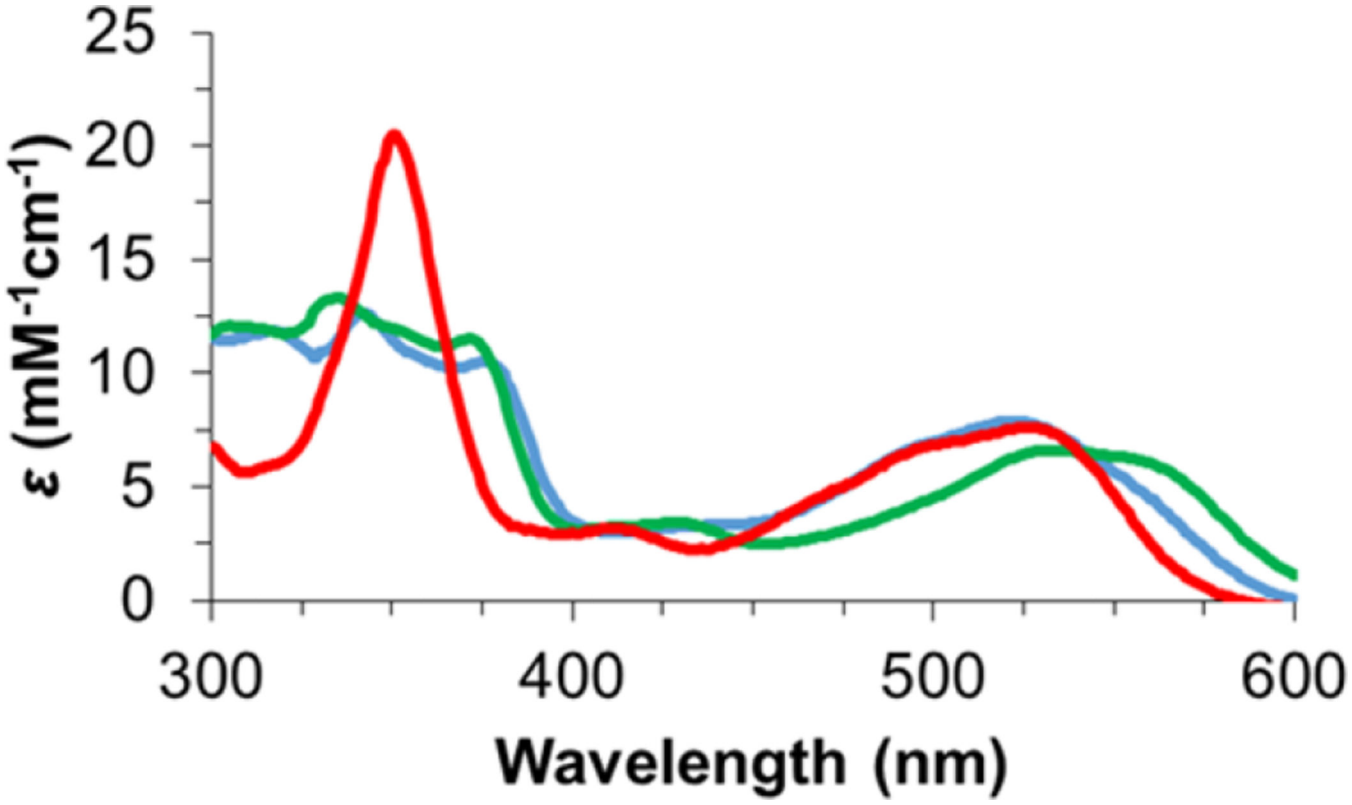

Figure 1.
Spectral overlay of **HOCbl** (red), **MeCbl** (blue), and NAcSCbl (green).

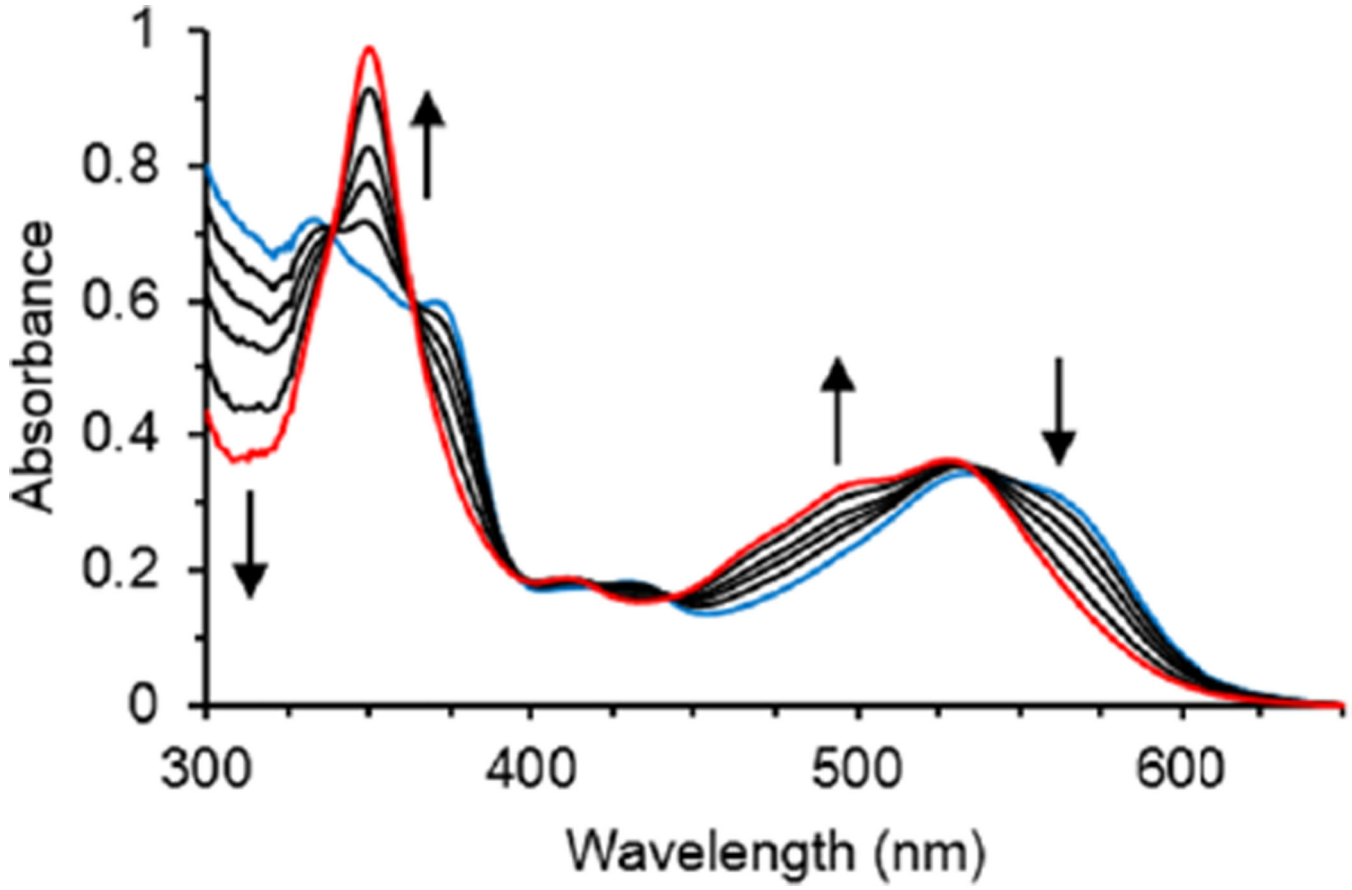

Figure 2.

Change in absorption due to photolytic (360 nm) conversion of **NAcSCbl** (blue line, 20 μM) to **HOCbl** (red line). Black lines indicate intermediate photolysis times of 1, 2, 3, and 4 min of the Cbl in acetate buffer (100 mM, pH 5.5).

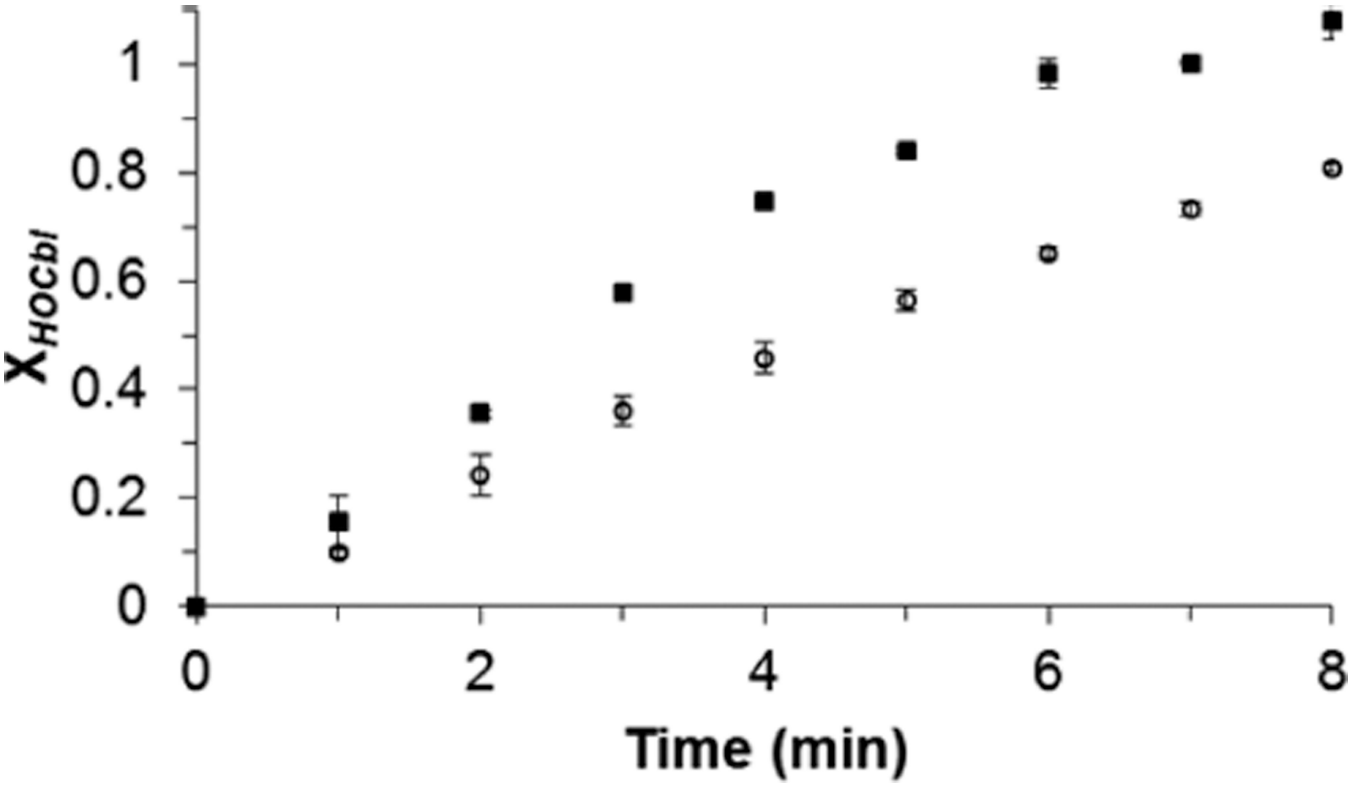

Figure 3.

Comparison of the photolytic conversion of **NAcSCbl** (open circles) and **NAcSCbl-2** (black squares) to **HOCbl** represented as the mole faction (X_{HOCbl}) versus illumination time (360 ± 10 nm).

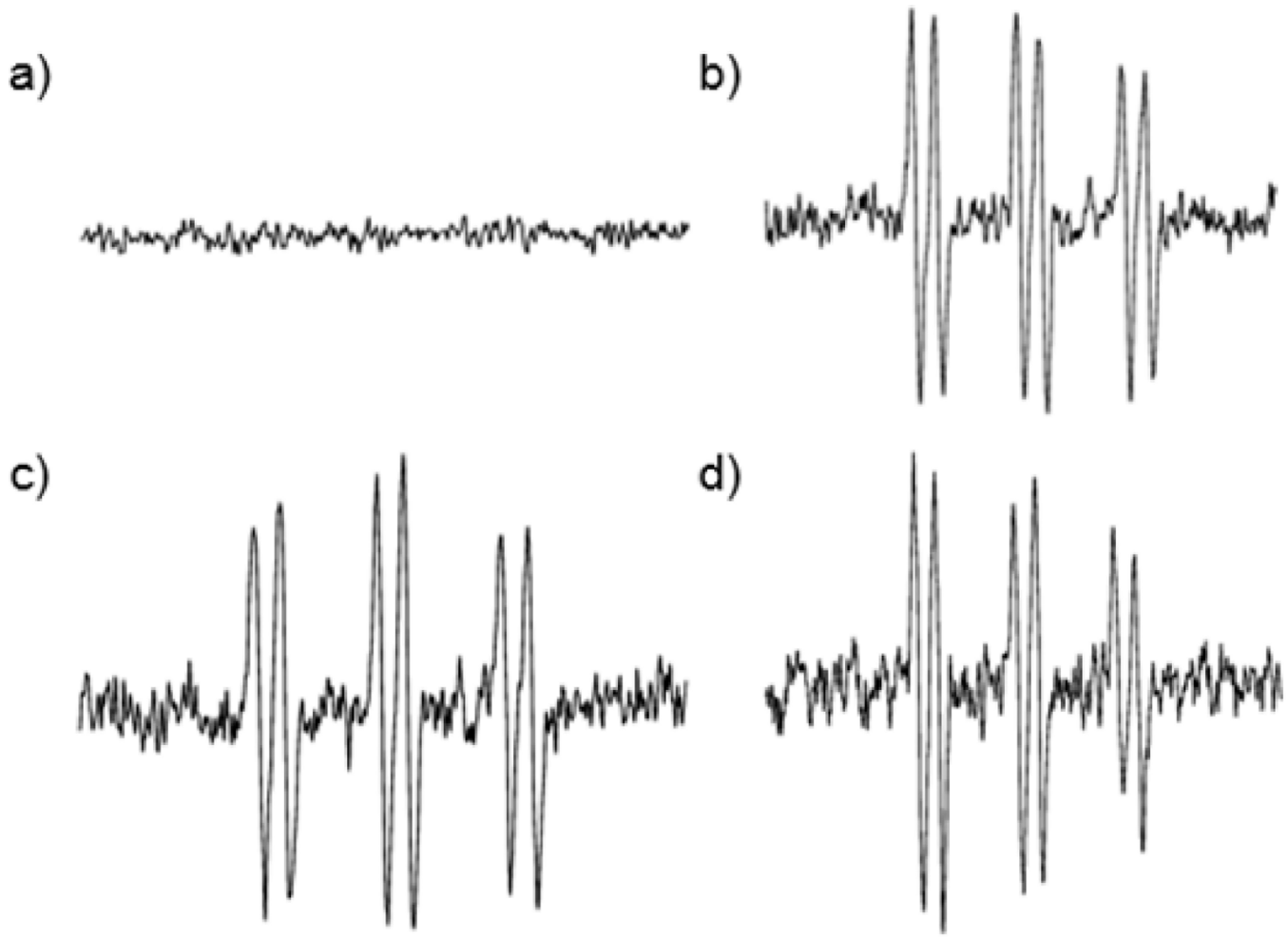

Figure 4.

EPR spectra of **NAcSCbl** (a) in the dark and (b) at 546 nm. (c) EPR spectrum of **NAcSCbl-4** at 546 nm. (d) EPR spectrum of peroxidase generated cysteinyl radical. PBN (100 mM) was used as the thiyl trap in the presence of **NAcSCbl** or **NAc-Cbl-4** (1 mM) in acetate buffer (100 mM, pH 5.5).

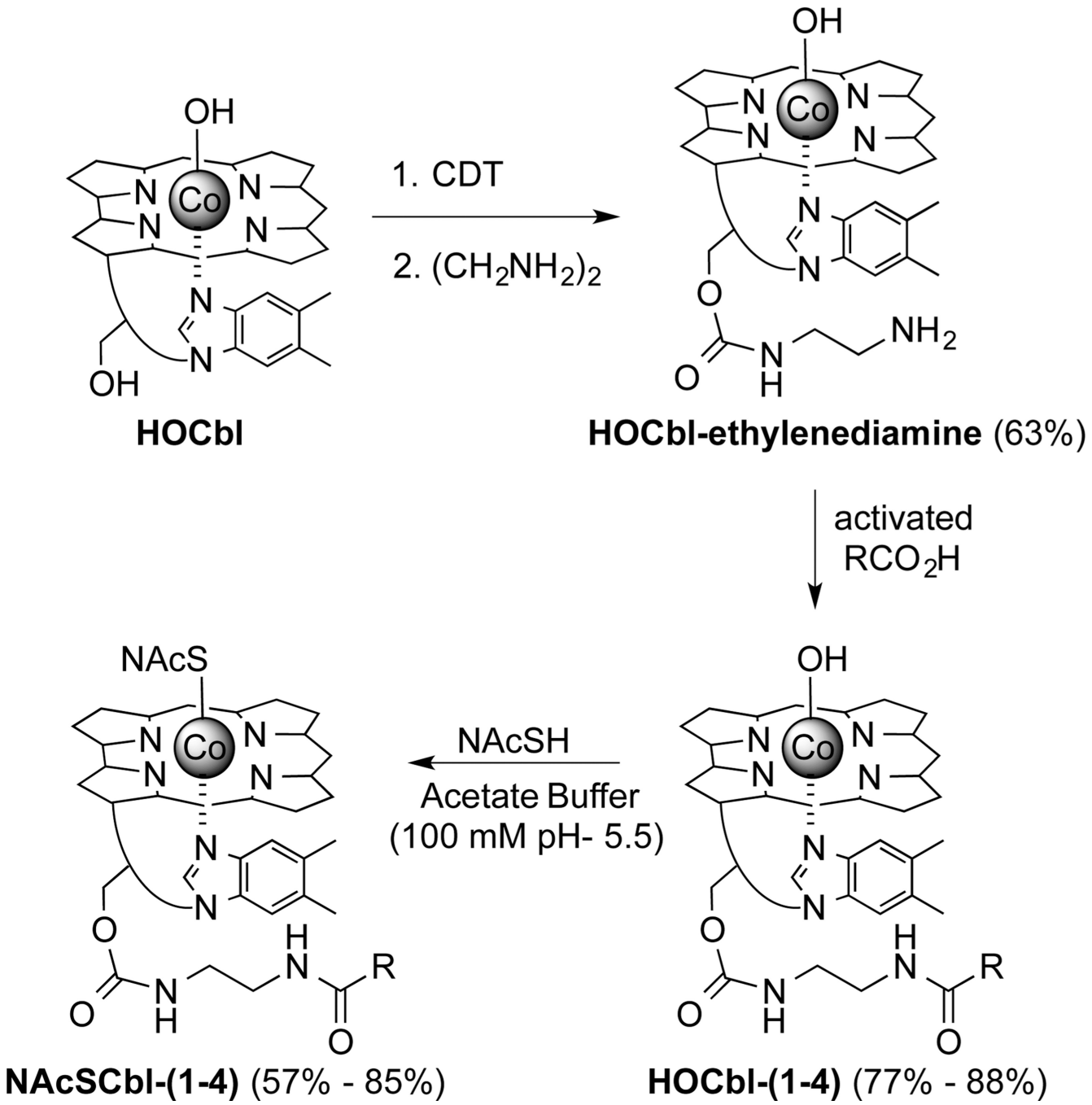

Scheme 1.

Synthesis of NAcSCbl Derivatives 1–4a

[a]Functionalization of **HOCbl** occurs via activation of ribose-5′-OH with CDT and subsequent treatment with ethylenediamine. Activated fluorophores can then be installed on the amine functional handle using NHS esters or uronium activators [**HOCbl-(1–4)**]. Finally, treatment of the constructs with **NAcSH** yields the desired thiolato-Cbls, where R: $–CH_3$ (**NAcSCbl-1**), –Alexa350 (**NAcSCbl-2**), –DEAC (**NAcSCbl-3**), and –TAMRA (**NAcSCbl-4**).

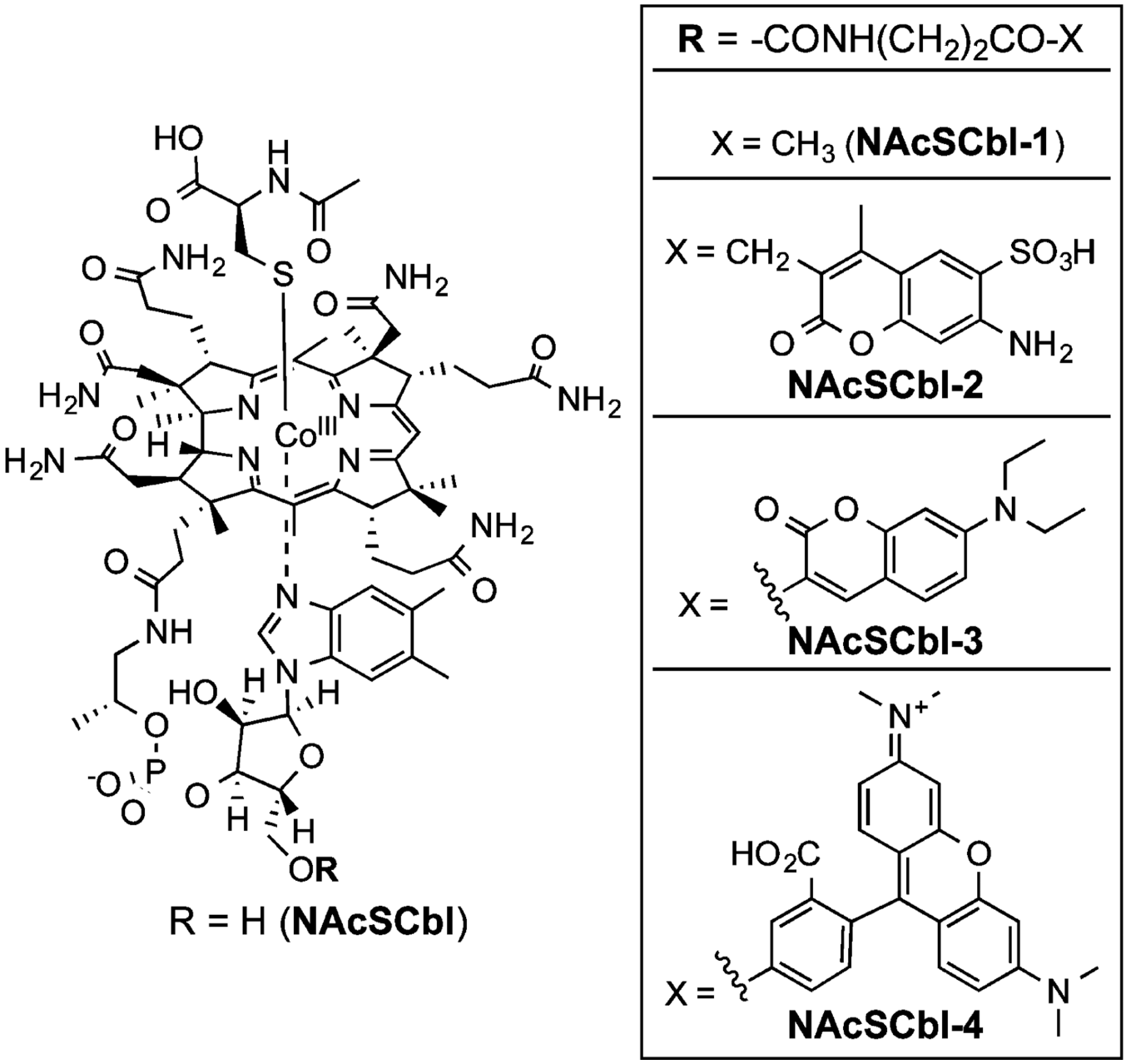

Chart 1.
Structures of NAcSCbl and Derivatives 1–4

Table 1

Quantum Yield (**Φ**), Extinction Coefficients (**ε**; M^{-1} cm^{-1}), Efficiency (**Φε**; M^{-1} cm^{-1}), and Normalized Rate Constants (*k*) for Photolysis of MeCbl and NAcSCbl

	λ (nm)[a]	**MeCbl**[b]	**NAcSCbl**
Φ[c]	360	0.30	(4.4 ± 0.8) × 10^{-4}
ε		10400	11400
Φε		3100	5.0 ± 1.0
k_{app}[d]		1.0 ± 0.2	(1.6 ± 0.3) × 10^{-3}
Φ[c]	405	0.30	(1.3 ± 0.1) × 10^{-4}
ε		3600	3300
Φε		1100	0.42 ± 0.02
k_{app}[d]		(3.0 ± 0.1) × 10^{-2}	(1.1 ± 0.1) × 10^{-5}
Φ[c]	546	0.15	(1.5 ± 0.1) × 10^{-5}
ε		6000	6400
Φε		900	0.10 ± 0.01
k_{app}d		0.13 ± 0.01	(1.5 ± 0.1) × 10^{-5}

[a] Hg lamp with band-pass filters (±10 nm).

[b] Literature Φ and ε are shown for **MeCbl**.[3]

[c] Calculated from eq 2.

[d] The constant was normalized to the rate of **MeCbl** at 360 nm where it cleaved fastest.

Table 2

Quantum Yield (**Φ**), Extinction Coefficients (**ε**; M^{-1} cm^{-1}), Efficiency (**Φε**; M^{-1} cm^{-1}), and Normalized Photolytic Rate Constants (*k*) of NAcSCbl-2, NAcSCbl-3, and NAcSCbl-4

	NAcSCbl-2 (360 ± 10 nm)[a]	**NAcSCbl-3 (405 ± 10 nm)[a]**	**NAcSCbl-4 (546 ± 10 nm)[a]**
Φ^b	$(3.4 \pm 0.6) \times 10^{-4}$	$(1.1 \pm 0.1) \times 10^{-4}$	$(9.2 \pm 0.5) \times 10^{-6}$
ε	27100	37800	84000
Φε	9.3 ± 1.7	4.2 ± 0.2	0.77 ± 0.04
$k_{app}{}^c$	$(3.0 \pm 0.6) \times 10^{-3}$	$(1.1 \pm 0.1) \times 10^{-4}$	$(1.1 \pm 0.1) \times 10^{-4}$

[a] Illuminated with Hg arc lamp source equipped with optical filters corresponding to the fluorophore's λ max (Alexa350 at 360 nm, DEAC at 405 nm, and TAMRA at 546 nm ±10 nm).

[b] Calculated from eq 2.

[c] The constant was normalized to the rate of **MeCbl** photolysis at 360 nm where it cleaved fastest.